Decolorization of Organic Dyes by Gold Nanoflowers Prepared on Reduced Graphene Oxide by Tea Polyphenols

M. Šimšíková[1⊠], M. Bartoš[1,2], J. Čechal[2], T. Šikola[1,2]

[1] CEITEC BUT, Brno University of Technology, Technická 10, 616 69 Brno, Czech Republic
[2] Institute of Physical Engineering, Brno University of Technology, Technická 2, 616 69 Brno, Czech Republic

INTRODUCTION

Majority of organic dyes that are used in various fields of industry and their products of degradation represent a serious environmental issue and potential hazard to living organisms.[1] Water soluble compounds, *e.g.* safranin T, eosin Y, and congo red (see Figure 1 for their chemical structure), are frequently used dyes with multitude industrial and medical applications. Safranin T is mainly used in textile industry, as the dye in flavoring and coloring candies and cookies in food industry, and in biological laboratories to identify Gram negative bacteria;[2] eosin Y is widely used in staining of differentiate bacterial species and proteins;[3] and congo red is extensively used as a synthetic organic dye in textile industry and in biochemistry and histology to stain microscopic preparates, especially as a cytoplasm and erythrocyte stain, and used as a sensitive diagnosis tool for amyloidosis.[4,5] However, each of the above mentioned dyes and their metabolites have significant harmful impact on the human and animal organisms and environment. Safranin T can cause the skin, respiratory tract and eye irritation[6] and it is dangerous to the aquatic organisms.[7] Eosin Y can cause skin and eye irritation with redness and pain, destroying retinal ganglion cell, injures the vital organs like liver and kidney on ingestion or lungs after the inhalation and it can also damages DNA in gastrointestinal organs of living beings.[8] Finally, the metabolites of congo red contain aromatic amine compounds which are highly harmful and carcinogenic for skin, eye, blood, bladder and reproductive cell of human body.[9,10]

Therefore, the treatment and removing of organic dyes from environment presents a very specific challenge. A wide range of physico-chemical and biological techniques, such as photodegradation, bio-degradation, precipitation methods, filtration, adsorption, and reverse osmosis have been investigated for elimination of dyes.[11] However, the conventional

----
⊠ Dr. Michaela Šimšíková, CEITEC BUT, Brno University of Technology, Technická 10, 616 69 Brno, Czech Republic
E-mail: michaela.simsikova@ceitec.vutbr.cz, Telephone number: +420 54114 2810

techniques are usually not as effective as required, and the degradation process often produces toxic or carcinogenic byproducts.

In recent years, the nanocatalysis has attracted considerable attention as a viable way of removing dyes and other organic pollutants from environment. It has been demonstrated that the application of metal nanoparticles is an excellent catalysts in organic synthesis reactions because of their very active surface atoms. In addition, the size, shape, surfactants, and supported substrates can positively affect catalytic efficiency of nanoparticles. Some recent works have been demonstrated the enhanced degradation of organic pollutants by nanoflowers due to their large surface to volume ratio and a high specific activity owing to high density of edge, corner, and step atoms present on their branches. The synthesis of flower-like nanoparticles can be divided to three main strategies – template-based method, assembling via oriented attachment of primary particles, and anisotropic growth which is induced by different capping agents.[12] Despite the large number of available synthesis methods, the employed chemical procedures may result in presence of toxic species adsorbed on the surface of nanostructures. Therefore, there is a growing need to develop environmentally benign procedures for nanoparticle synthesis that do not use toxic chemicals in the synthesis protocols. Recently, application of some natural reducing agents such as amino acids,[13] enzymes,[14,15] saccharides,[16,17] plant extracts,[18] and bacteria[19] for formation of nano-gold have been studied. However, very little attention has been given to the preparation of gold flower-like nanostructures.[12,20,21]

In this paper we describe a simple, efficient, and green strategy for the synthesis of gold flower-like structures by assembling nanoparticles on reduced graphene oxide surface in the presence of green tea. The preparation of rGO by tea polyphenols has been already studied;[22,23] nevertheless, the synthesis of gold nanoflowers attached on rGO by this procedure has not yet been described. Even though the graphene based materials are considered to be good photocatalysts,[24-27] we have shown that there was almost no effect of rGO on dye decolorization without external illumination (Fig. S1, S2). Therefore, we can assume that the degradation of three well-studied organic dyes (congo red, safranin T, and eosin Y) described in presented study is caused by gold nanoflowers and the graphene oxide served prevalently as a substrate for successful formation of branched nanostructures. We demonstrate that our complex enhances the rate at which the reductant decomposes the examined dyes.
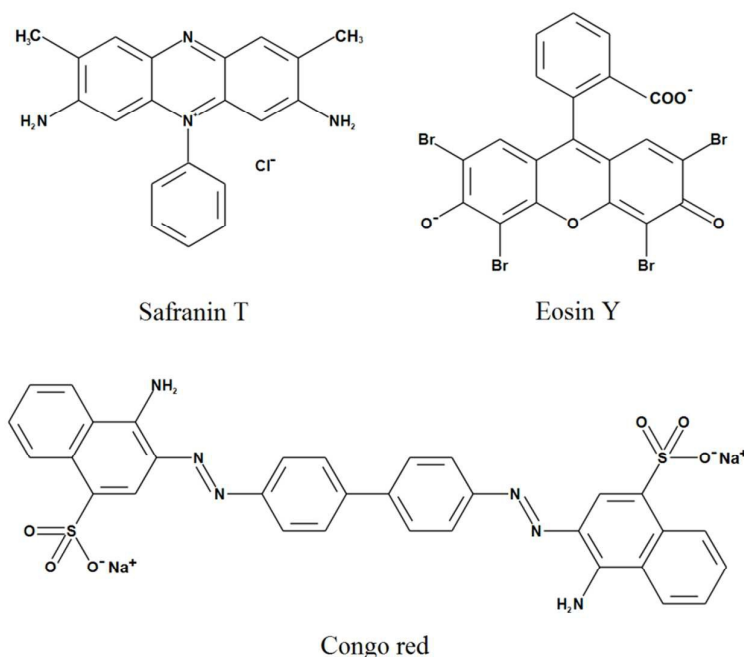
Figure 1 Chemical structure of safranin T, eosin Y, and congo red.

RESULTS AND DISCUSSION

We have recently reported on the formation of spherical gold nanoparticles on rGO employing green tea as a reducing agent and described in detail the morphology and optical properties of formed nanoparticles.[28] After the slight adaptation of procedure we were able to obtain nanoparticles with flower-like morphology. The magnified view of prepared rGO-AuNFs nanocomposite presented in the Figure 2c reveals that the formation of small gold nanoparticles comprises several intercepting gold sheets with lateral size (200-400 nm and thickness below 20 nm) which can be explained by the strong interaction between gold nanoparticles and reduced graphene oxide. The same preparation procedure in identical conditions, except for presence of rGO, leads to the formation of spherical nanoparticles (Figure 2b); it shows the significant role of graphene oxide surface in formation of branched gold nanostructures. Similar behavior has been observed for CuO nanoparticles after their assembly on the graphene oxide.[29] However, based on literature and our previous work we can conclude that the morphology is strongly influenced by concentration ratio between precursor and reductant, as well.[28,30] Addition of same amount of reducing agent and a lower concentration of gold salt favors the formation of nanospheres with diameter approximately ~20-40 nm, while the higher concentration of gold salt leads to the formation of higher amount of the nanospheres which are subsequently assembled as nanoflowers.[28]
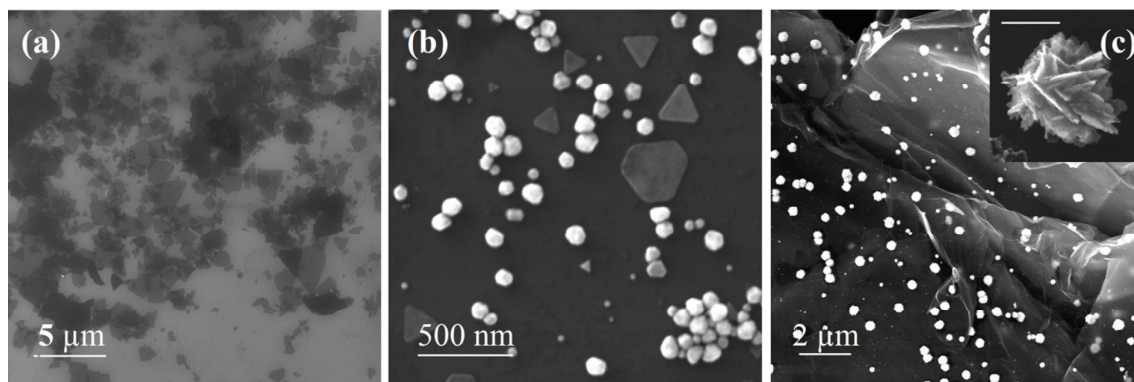
Figure 2 Scanning electron micrographs of a graphene oxide (**a**), gold nanoparticles (**b**), graphene oxide decorated by gold nanoflowers (**c**), and AuNF on rGO in a higher magnification (**c**, *inset*; bar 100 nm). All of the samples have been prepared in the presence of green tea.

Raman spectroscopy is one of the most widely used techniques to characterize carbonaceous materials, particularly to see the difference between disorder and defect structures, defect density, and doping levels. It is well known that Raman spectrum of graphene exhibits two characteristic peaks, the *D* band approximately at 1350 cm^{-1} arising from a breathing mode of Қ-point photons of A_{1g} symmetry, and the *G* band at 1575 cm^{-1} due to the first order scattering of the E_{2g} photon of sp^2 *C* atoms.[31,32]

In our study, Raman spectra were used to analyze significant structural changes occurring during the reduction process from GO to rGO and after the deposition of gold on rGO surface. The spectrum of graphene oxide after the reduction by green tea exhibits the typical features of carbon, the *D* and *G* bands at 1353 and 1607 cm^{-1}, respectively (Figure 3a, *purple line*). The change of place and ratio of relative intensities of the *D* peak and *G* peak in the Raman spectra of graphene oxide after the application of green tea as a reductant indicate a change in the electronic conjugation state. This change suggests an increase in the number of sp^2 domains following reduction of GO.[33]

Raman spectrum of rGO-AuNFs is characterized by the increasing intensity of *D* and *G* bands (1353 and 1606 cm^{-1}) (Figure 3a, *green line*) which can be attributed to the dramatic Raman enhancement after the creation of gold nanoparticles.[34]

Figure 3b represents the FTIR spectra of graphene and its functionalized products. The spectrum of as-prepared graphene oxide (*pink line*) shows a broad absorption band located at about 3290 cm^{-1} due to O-H vibrations of intercalated water or carboxylic acid, respectively. The band located at 2924 and 2850 cm^{-1} can be assigned to the stretching vibrations v_{as} (C-H) and v_s (C-H) of alkane groups. The signal at 1740 cm^{-1} is arising from the C=O

carbonyl/carboxyl bands, and the peak at about 1590 cm^{-1} corresponds with the C=C aromatic stretch. Stretching deformation vibrations of water and skeletal vibrations of unoxidized graphitic domains were reflected as band approximately at 1630 cm^{-1}.[35]

The spectrum of rGO reveals the absence of absorption band for OH vibrations and the decreasing of signal for C=O, as well. These changes indicate the successful reduction of graphene oxide which is in good agreement with other authors.[36,37] In FTIR spectrum of rGO-AuNFs, the intensity of characteristic features for rGO were increased and slightly shifted to the lower value which can be assigned to the formation of gold nanoparticles on rGO surface.[38]

Figure 3c presents the survey XPS spectra of GO, rGO, and rGO-AuNFs. The peaks at binding energies centered at 531.1 eV and 282.7 eV are associated with C 1s and O 1s core levels, respectively. The decrease in the intensity of O 1s peak after the GO reduction (cf. GO and rGO spectra) indicates the loss of oxygen and successful implementation of this procedure. After the formation of gold nanoflowers on surface of reduced graphene oxide a new peak associated with Au 4f core levels (84.0 eV) proves the successful decoration of rGO with gold.
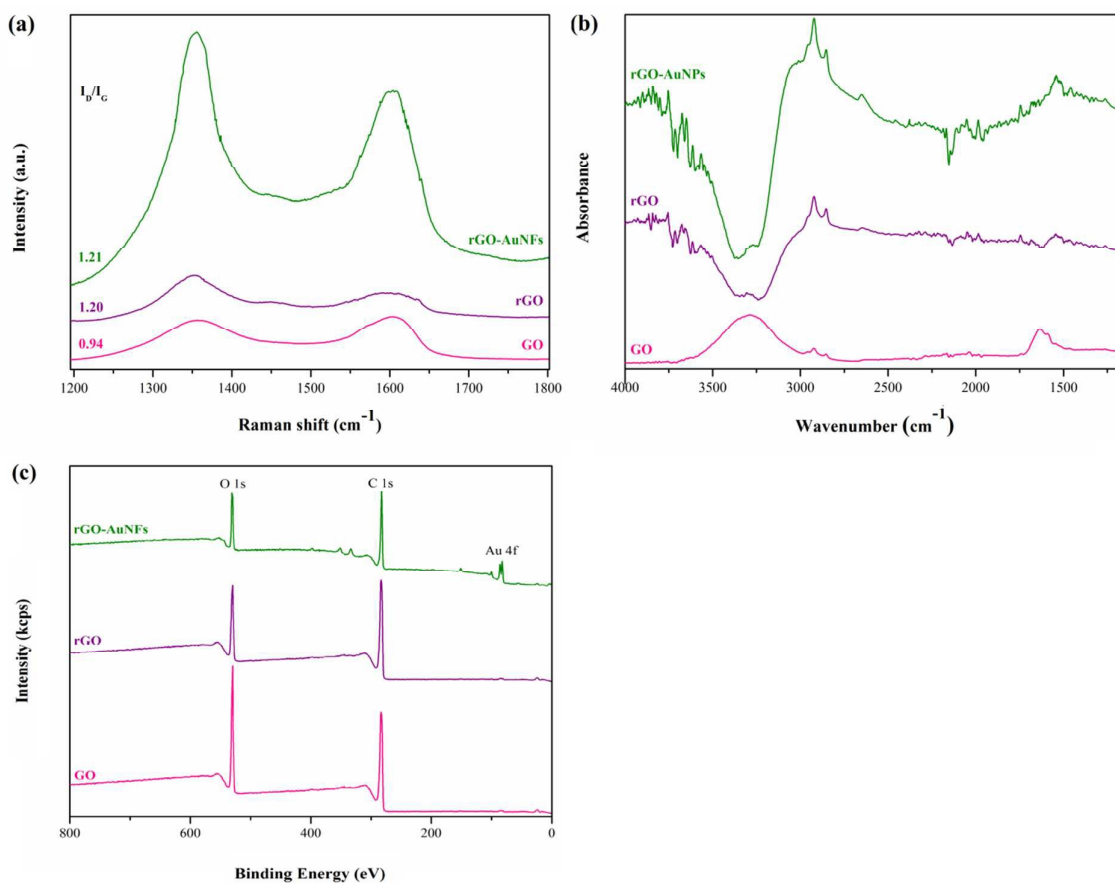
Figure 3 Raman (**a**), FTIR (**b**), and XPS survey spectra (**c**) of as-prepared GO (*pink line*), GO reduced by green tea (*purple line*), and rGO-AuNFs complex (*green line*).

Graphene-based materials have been described as a very good photocatalyst in degradation of various dyes[24-26] due to their ability to act as an excellent electron-acceptor for effective facilitation of the migration of photo-induced electrons and barrier of charge recombination in electron-transfer process which enhances photocatalytic performance.[27] In spite of this, in this work we describe the catalytic activity of gold nanoflowers in degradation of three well-studied organic dyes (congo red, safranin T, and eosin Y) without the presence of light; the graphene oxide serves only as a substrate for successful formation of branched nanostructures.

Above mentioned dyes can be reduced by reductants like sodium borohydride to form small organic molecules firstly and non toxic species finally, but the reduction rate is very slow (see Supplementary Information). Metal nanoparticles can accelerate the reduction rate of dyes and increase the reducing efficiency due to their high reactive activity and specific surface area. Metal nanoparticles act as an electron relay and electron transfer occurs via nanoparticles from BH_4^- to dye molecules. Nucleophilic borohydride ions can donate

electrons to metal particles, while electrophilic dyes would capture electrons from nanoparticles. The electron transfer affects the chemical nature of organic dyes and causes their cleavage into smaller non-toxic molecules.[39,40] The acceleration of degradation of various compounds by mentioned principle has been reported in various research works. Jiang et al.[40] demonstrated the catalytic properties of silver nanoparticles supported on silica spheres toward the various organic dyes. Narayanan and Sakthivel[41] described preparation of nano-gold composite for its successful catalytic application in the degradation of 4-nitrophenol in the presence of sodium borohydride.

Figure 4 shows a series of UV–Vis absorption spectra of degradation of dyes by $NaBH_4$. The presence of the dye in solution can be monitored by intensity of absorption peak associated with studied dyes. For blank experiments, in the absence of the catalyst, almost no degradation of the safranin T took place (Figure S3a in Supplement Inofrmation). In contrast, in the presence of rGO-AuNFs without irradiation, the full decolorization was observed within 10 min. The rate of eosin reduction in the absence of catalyst was very slow and took 63 min (Figure S3b in Supporting Information) whereas the addition of rGO-AuNFs reduced the reaction time to less than 18 min indicating the acceleration of the reaction by nanocatalyst (Figure 4b). The decolorization activity of the congo red using gold nanoflowers assembled on the graphene oxide surface was studied, as well. After the addition of rGO-AuNFs, the considerable decreasing of the absorption was observed which indicates the positive effect of composite to the progress of reduction reaction. The whole process of dye degradation was finished after 26 min (Figure 4c).

Compared with spherical gold nanoparticles assembled on surface of rGO, the recent results indicate that gold nanoflowers exhibit higher catalytic effect.[28]
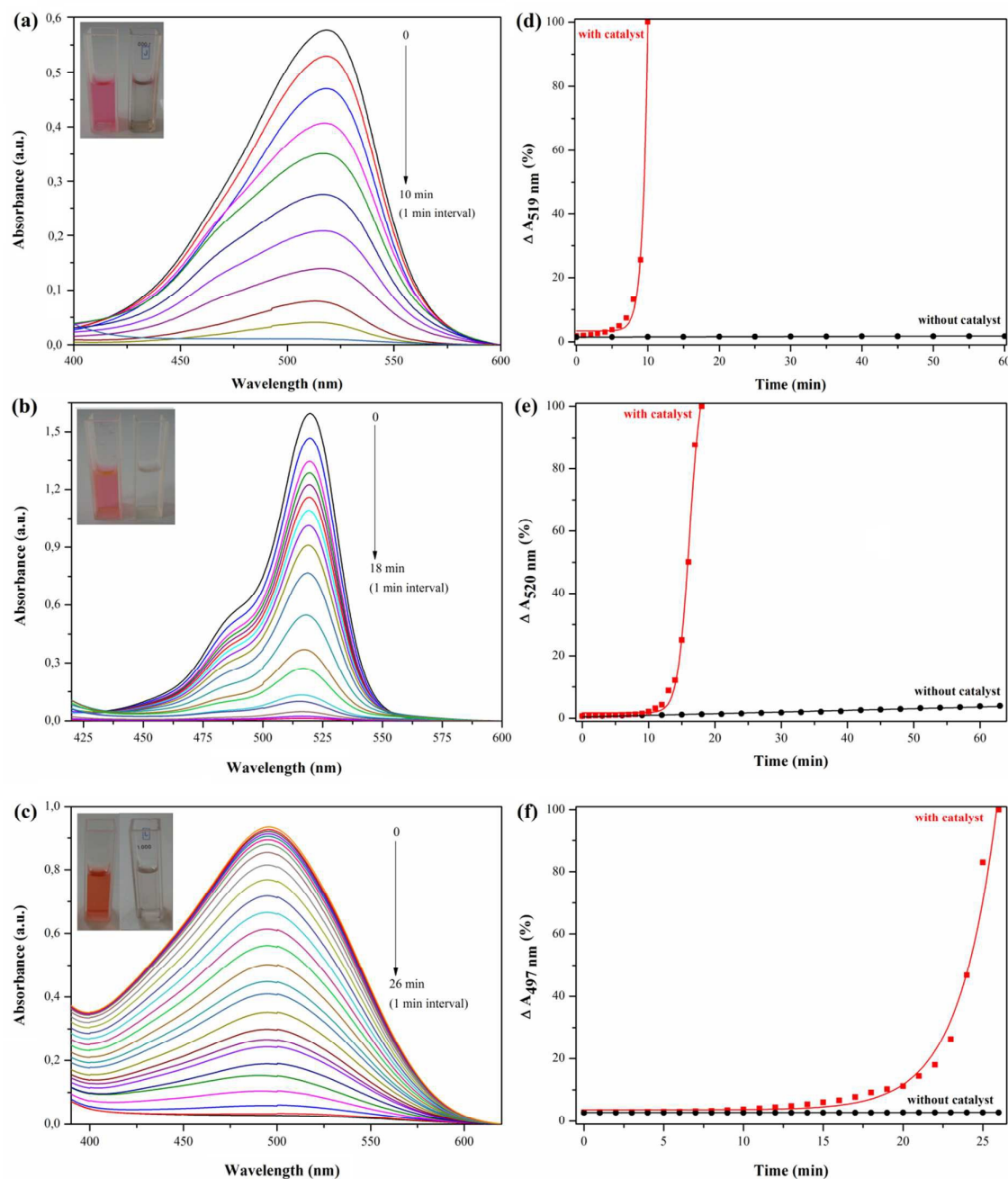
Figure 4 UV-Vis absorption spectra of the borohydride reduction of safranin T (**a**), eosin Y (**b**), and congo red (**c**) catalyzed by rGO-AuNFs composite. The plot of the absorbance at λ_{max} of appropriate dye in the presence of NaBH$_4$ with and without catalyst versus time: safranin T (**d**), eosin Y (**e**), and congo red (**f**).

The measurement of fluorescence is not so commonly used method for determination of dye degradation. Nevertheless, the obtained results can bring complementary information on the molecular and structural changes of safranin T, eosin Y, and congo red during degradation. The emission spectra of safranin T solution after the addition of the catalyst

8

display only slight changes up to 11 min as depicted in Figure 5a. Within this time interval, the emission peak moved slightly from 582 nm to 580 nm and its intensity decreased by 29 %. After this time, the reduction reaction proceeded much more progressively. The peak position was further shifted to 572 nm while its intensity rapidly decreased. Within 15 min, the emission peak diminished which indicates the complete decolorization of dye.[42]

The reduction process of eosin Y was studied by determination of change in fluorescence of the initially observed peak at 613 nm (Figure 5b). Upon the time, the position of emission peak gradually blue shifted. The limit position of peak was approximately at 553 nm after 18 min of exposition of reductant in the presence of rGO-AuNFs as a catalyst. Subsequently, the emission spectrum of eosin Y exhibits only the residual fluorescence of dye.[43]

Finally, emission spectra of the congo red in the presence of $NaBH_4$ and rGO-AuNFs showed a gradual shift from the original position approximately at 610 nm to final value at 597 nm (Figure 5c). Here, the fluorescence quenching effects characterized by less defined shape of the emission peak were observed, as well. Mentioned changes indicate the successful decolorization of congo red.

The interaction of fluorophore with various compounds can be followed by shifting of emission band and decreasing of fluorescence intensity. The fluorescence decline can be attributed to the quenching of electron singlet excited state, through non-radioactive transition back to the ground state as a consequence of energy transfer or electron transfer in associated with the property of the fluorophore, conjugation mode, and local environment.[44,45] Several examples of excited state quenching of organic dyes have been reported. Liu et al.[46] used graphene and graphite oxide as an effective quencher for three different organic dyes. Huang and Murray[47] demonstrated the quenching of small molecule dyes by gold nanoparticles, and Bera et al.[48] described the formation of complex between rhodamine B and gold nanoflowers which was accompanied by rapid quenching of dye fluorescence intensity and a blue shift of its emission maximum.

In our system, the interaction between the excited dyes and reducing agent ($NaBH_4$) and the subsequent disruption of the conjugated system caused a decrease in absorbance / fluorescence of the dyes as a consequence of interfacial charge-transfer process. However, the uncatalyzed reaction showed only a small percentage of dye decolorization which suggests that the electron transfer process is insufficient (Figure S3, S4 Supplementary Information). On the other hand, the more significant absorption / emission change after the introduction of rGO-AuNFs to the system indicates that nanoflowers on GO-substrate act as an efficient catalyst through the electron transfer process. In summary, the whole changes in absorption /

emission spectra of dyes can be explain by the four steps: (1) dyes are adsorbed onto the rGO-AuNFs surface by electrostatic interaction; (2) electrons transferred from BH_4^- to gold nanoflowers are moved to the dye molecules; (3) electrophilic dyes capture electrons from metal particles; and finally (4) the electron transfer causes interruption of double bonds in conjugated systems of safranin T and eosin Y and chemical cleavage of congo red, respectively (see Scheme 1).[38,40,49-53]

Whereas many research groups have reported the use of rGO as effective adsorbent materials for organic dyes,[54-56] the adsorptive activity of rGO and rGO-AuNFs toward the dyes should be considered, as well. The affinity of graphene oxide based materials can be mainly attributed to the large surface area, the oxygen-containing functional groups such as hydroxyl, carboxylic, carbonyl, and epoxy groups, the aromatic matrix, and high water solubility. The favorable interaction between organic dyes and graphene oxide is based on electrostatic interactions or forming of hydrogen bonds at hydrophilic species; π-π stacking or hydrophobic interactions between hydrophobic species, respectively.[54-56] However, our experiments of dye decolorization in the presence of rGO and rGO-AuNFs showed no significant changes which indicates nonexistent or very low adsorption of dyes on the graphene oxide (Fig. S1, S2, and S5). These differences compared with results of other authors can be caused by different experimental conditions such as lower concentration of rGO in system and shorter contact time. The authors have demonstrated the effect of pH and temperature, as well.[55,57] These parameters may also play significant role in lower adsorption of dyes on graphene oxide surface. Based on these results we can infer that the decolorization of dye solutions was mainly caused by effect of the reductant agent ($NaBH_4$) in the presence of GO-AuNFs as a catalyst.
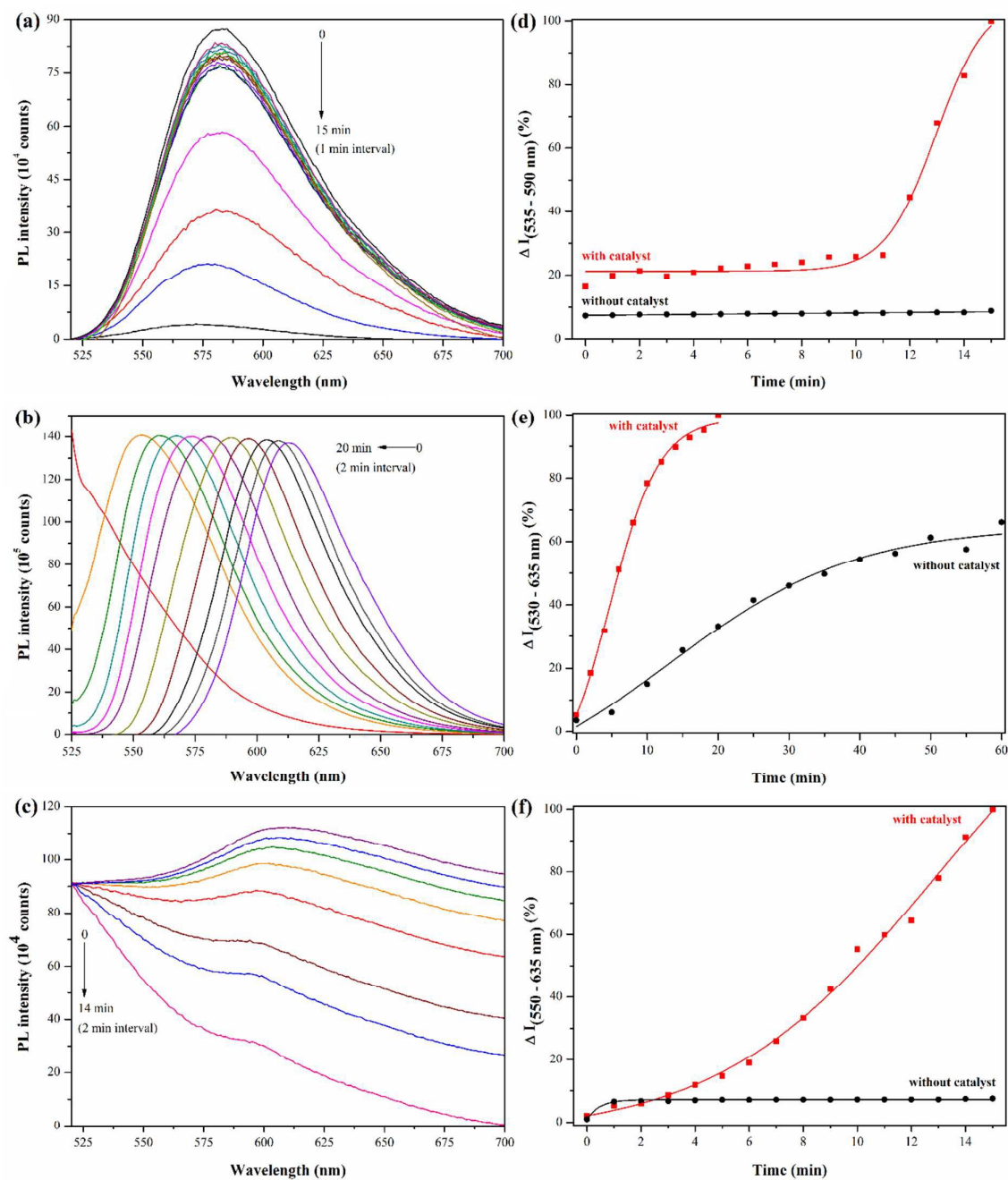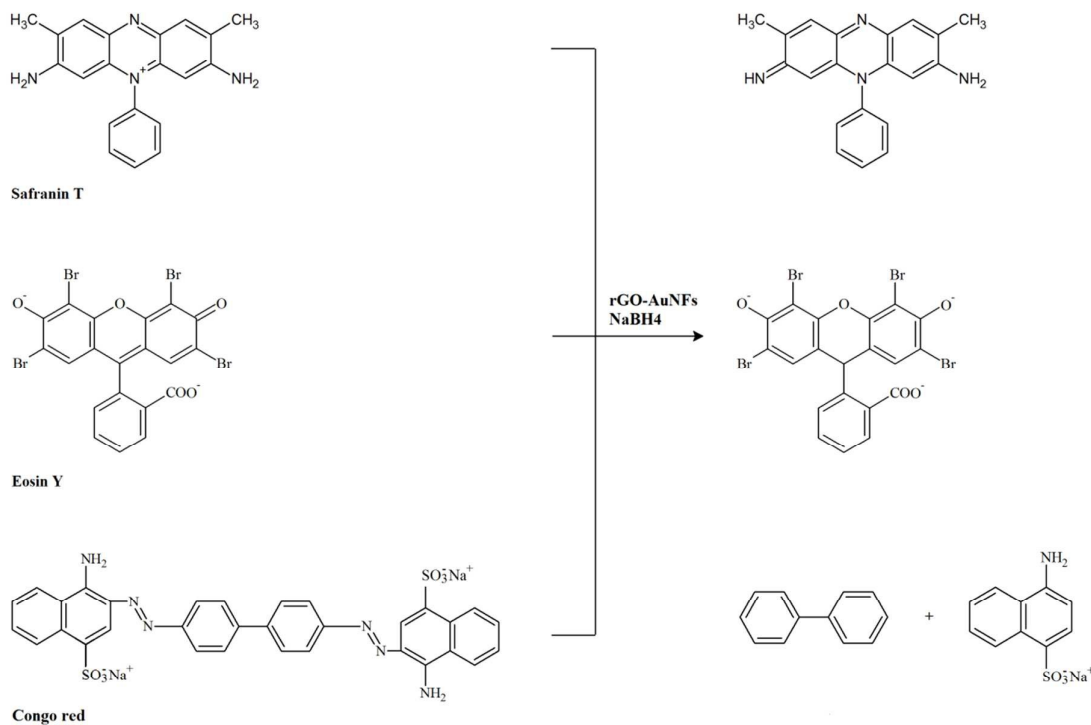
Figure 5 Emission spectra of dye degradation at various reaction times in the presence of rGO-AuNFs composite: safranin T (**a**), eosin Y (**b**), and congo red (**c**). The plot of the fluorescence of dye in the presence of NaBH$_4$ with and without catalyst versus time: safranin T (**d**), eosin Y (**e**), and congo red (**f**).

11

Scheme 1 Possible products of decolorization of safranin T, eosin Y, and congo red by NaBH$_4$ in the presence of rGO-AuNFs as a catalyst.

EXPERIMANTAL

Materials

Graphite powder (NGS Naturgraphit GmbH, Germany) was used as received. Sulfuric acid (H$_2$SO$_4$, 95.0-98.0%), potassium permanganate (KMnO$_4$, ≥99.0%), sodium nitrate (NaNO$_3$, ≥99.0%), hydrogen peroxide solution (H$_2$O$_2$, ≥30%), and gold(III) chloride trihydrate (HAuCl$_4$.3H$_2$0, ≥99.9%) were purchased from Sigma Aldrich (USA). For determination of catalytic activity of rGO-AuNFs was used sodium borohydride (NaBH4, 99.99%) from Sigma Aldrich (USA) as a reductant and organic dyes - safranin T (C$_{20}$H$_{19}$ClN$_4$, Fluka, Germany), eosin Y (C$_{20}$H$_6$Br$_4$Na$_2$O, Penta, Czech Republic), and congo red (C$_{32}$H$_{22}$N$_6$Na$_2$O$_6$S$_2$, Sigma Aldrich, USA).

We have applied modified Hummers method for preparation of graphene oxide powder.[58] Obtained sample was collected by centrifugation (Minispin Eppendorf; 30 min, 12 000 rpm, 25°C) and washed several times by ultrapure water for removing of unexploited graphite and subsequently dried at 80°C.

The green tea extract was prepared by leaching 1.2 g of green tea powder (95% purity, purchased in special tea market) in 10 mL of ultrapure water (80°C) for 5 min. The extracted solution was then filtered twice through a 0.22 μm cellulose membrane and cooled at room temperature to obtain a clear solution of the infused green tea with honey color.

Ultrapure water was used throughout the course of investigation.

Synthesis of rGO-AuNFs

The reduction of GO and subsequent formation of gold nanoflowers on its surface was performed by mixing 25 mL of GO suspension (1 mg / 1 mL) with an aqueous solution of $HAuCl_4$ (12.5 mL, 2 mM) by vortex mixer (IKA Werke, Germany) for 2 min. Subsequently, 1 mL of tea extract was added drop by drop to the solution at room temperature. Resulted solution was left in dark for 24 h. After that, solution was collected by centrifugation (Eppendorf 5804R centrifuge; 5 min, 15 000 rpm, 25°C) and washed with ultrapure water several times to remove of unassembled nanoparticles and then redispersed in 25 mL of ultrapure water.

Reduced GO was prepared by similar procedure as rGO-AuNFs without the presence of gold salt. Gold nanoparticles were prepared by mixing 25 mL of ultrapure water with 12.5 mL of 2 mM $HAuCl_4$ salt and subsequent reduction by 1 mL of green tea extract.

Characterization of rGO-AuNFs

Raman spectra of GO, rGO, and rGO-AuNFs were performed using an optical tweezer consisting of a trapping fiber laser IPG YLM-10-LP-SC (IPG Photonics, Japan) with maximal output power of 10 W at 1070 nm and Spatial Light Modulator X10468-03 (Hamamatsu, Japan) combined with the micro-Raman spectrometer Shamrock SR 303i (Andor, England) and the low noise camera Newton DU970P (Andor, England). The Raman spectra were excited by 532 nm laser torus 532 + mpc 3000 (Laser Quantum, England) with applied power of around 320 mW; the trapping of prepared complexes was performed using the 1.5 W power IPG laser and active output. All spectra were measured from 500 to 2 200 cm^{-1} after the dispersion in ultrapure water and subsequently deposited on glass slides. The spectra were initially calibrated by 4.5 μm polystyrene latex beads and gave the resolution at peak positions of less than 1 cm^{-1}.

Infrared ATR spectra were carried out with a Nicolet 8700 Fourier transform infrared spectrometer (Thermo Scientific, USA) equipped with Smart OMNI-Sampler (diamond crystal), deuterated triglyceride sulfate (DTGS) detector and a KBr beamsplitter. All spectra

were collected for 64 scans at a resolution of 4 cm^{-1} in range of 4000-400 cm^{-1} with a 150 cm^{-1} aperture. Spectra referenced to the air served as a background spectrum previously recorded on the crystal without the samples.

X-ray photoelectron spectroscopy was performed using Kratos Axis-Ultra DLD system using monochromatic Al-Kα radiation with automatic charge compensation turned on.

Scanning Electron Microscope LYRA 3 XMU (Tescan, Czech Republic) was used to determinate the successful formation of gold nanoflowers on graphene oxide surface. Voltage of 30 kV was used during all the experiments.

Catalytic activity of rGO-AuNFs

The catalytic activity of gold nanoflowers assembled on graphene oxide toward the organic dyes (safranin T, eosin Y, and congo red) was studied by absorption and fluorescence method which were carried out using a UV-Vis spectrophotometer V-630 (Jasco, Japan) and FluoroMax-4 spectrofluorometer (Horiba Jobin Yvon, Japan) equipped with Xe lamp, respectively. A 1.00 cm path length rectangular quartz cell was used for each absorption and fluorescence measurements.

2 mL of ultrapure water was mixed with 10 µL (for absorption measurements) or 5 µL (for PL measurements) of 0.01 M solution of appropriate dye in a 1.00 cm path length quartz cell. Then 100 µL of 0.1 M NaBH$_4$ was added to the prepared solution. Finally, 10 µL of graphene oxide decorated by gold nanoflowers was added to the solution. The progress of reduction was monitored in situ monitoring a UV-Vis spectrophotometer and photoluminescence spectrofluorometer, as well. Emission spectra for dyes were measured after the excitation at 510 nm, 520 nm, and 497 nm with 2 nm, 5 nm, and 7 nm emission and excitation slit for safranin T, eosin Y, and congo red, respectively.

Each of absorption and fluorescence measurements has been repeated three times.

CONCLUSION

Polyphenols from green tea extract have been used for a one-step a green approach for preparation of well-defined flower-like gold nanostructures which were uniformly supported on rGO. Presented method did not require the use of any surfactants or seeds. Highly branched nanoflowers characterized by sheets with lateral size ~200-400 nm and thickness below 20 nm have been formed by oriented attachment of primary particles due to the strong interaction between gold nanoparticles and reduced graphene oxide surface.

The dye degradation of safranin T, eosin Y, and congo red has been investigated in electron transfer from borohydride via gold nanoflowers formed on rGO without light irradiation. The results show that application of rGO-AuNFs significantly enhanced the degradation of selected organic dyes.
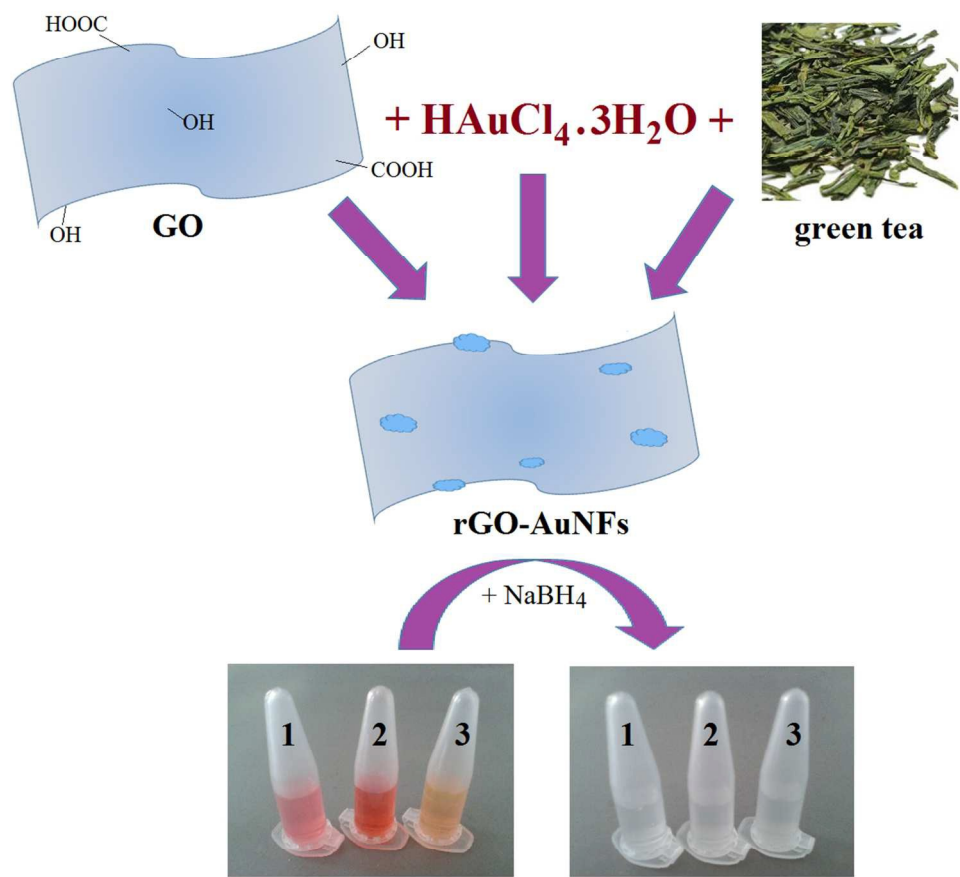
REFERENCES

1. A. Bafana, S.S. Devi and T. Chakrabarti, *Environ. Rev.,* 2011, **19**, 350-370.

2. V.K. Gupta, A. Mittal, R. Jain, M. Mathur and S. Sikarwar, *J. Colloid Interface Sci.,* 2006, **303**, 80-86.

3. G.A. Johnson, N. Muthukrishnan and J.P. Pellois, *Bioconjugate Chem*., 2013, **24**, 114-123.

4. S.B. Yamaki, D.S. Barros, C.M. Garcia, P. Socoloski, O.N. Oliveira and T.D. Atvars, *Langmuir*, 2005, **21**, 5414-5420.

5. A.K. Schutz, A. Soragni, S. Hornemann, A. Aguzzi, M. Ernst, A. Bockmann and B.H. Meier, *Angew. Chem. Int. Ed*., 2011 **50**, 5956-5960.

6. V. Janaki, B.T. Oh, K. Shanthi, K.J. Lee, A.K. Ramasamy and S. Kamala-Kannan, *Res. Chem. Intermediat*., 2012, **38**, 1431-1442.

7. V.K. Gupta, A. Mittal, R. Jain, M. Mathur and S. Sikarwar, *J. Colloid Interf. Sci.,* 2006, **303**, 80-86.

8. A. Mittal, D. Jhare and J. Mittal, *J. Mol. Liq.*, 2013, **179**, 133-140.

9. V.A. Sakkas, A. Islam, C. Stalikas and T.A. Albanis, *J. Hazard. Mater.*, 2010, **175**, 33-44.

10. O. Mohanta, Y.N. Singhbabu, S.K. Giri, D. Dadhich, N.N. Das and R.K. Sahu, *J. Alloy. Compd.,* 2013, **564**, 78-83.

11. Y.M. Slokar and A. Majcen Le Marechal, *Dyes Pigment.*, 1998, **37**, 335-356.

12. L. Li and J. Weng, *Nanotechnology*, 2010, **21**, 305603.

13. N. Wangoo, K.K. Bhasin, S.K. Mehta and C. Suri, *J. Colloid Interface Sci.,* 2008, **323**, 247-254.

14. K. Kalishwaralal, S. Gopalram, R. Vaidyanathan, V. Deepak, S.R.K. Pandian and S. Gurunathan, *Colloid Surf. B,* 2010, **77**, 174-180.

15. H. Kawasaki, K. Hamaguchi, I. Osaka and R. Arakawa, *Adv. Funct. Mater*., 2011, **21**, 3508-3515.

16. Z.M. Qi, H.S. Zhou, N. Matsuda, I. Honma, K. Shimada, A. Takatsu and K. Kato, *J. Phys. Chem. B*, 2004, **108**, 7006-7011.

17. D.R. Bhumkar, H.M. Joshi, M. Sastry and V.B. Pokharkar, *Pharm. Res*., 2007, **24**, 1415-1426.

18. M.N. Nadagouda and R.S. Varma, *Green Chem.*, 2008, **10**, 859-862.

19. A.K. Suresh, D.A. Pelletier, W. Wang, M.L. Broich, J.W. Moon, B. Gu, D.P. Allison, D.C. Joy, T.J. Phelps and M.J. Doktycz, *Acta Biomater.*, 2011, **7**, 2148-2152.

20. D. Sun, G. Zhang, J. Huang, H. Wang and Q. Li, *Materials*, 2014, **7**, 1360-1369.

21. C. Lv, X.Y. Zhang, C.L. Mu, D. Wu, C.M. Wang and Q.L. Zhang, *J. Nanosci. Nanotechnol.*, 2015, **15**, 2761-2769.

22. Y. Wang, Z.X. Shi and J. Yin, *ACS Appl. Mater. Interfaces*, 2011, **3**, 1127–1133.

23. S. Thakur and N. Karak, *Carbon*, 2012, **50**, 5331-5339.

24. H. Zhang, P. Xu, G. Du, Z. Chen, K. Oh, D. Pan and Z. Jiao, *Nano. Res.*, 2011, **4**, 274-283.

25. S. Liu, W. Peng, H. Sun and S. Wang, *Nanoscale*, 2014, **6**, 766-771.

26. J. Zhang, Z. Xiong and X.S. Zhao, *J. Mater. Chem.*, 2011, **21**, 3634-3640.

27. S. Morales-Torres, L.M. Pastrana-Martinez, J. L. Figueiredo, J.L. Faria and A.M. Silva, *Environ. Sci. Pollut. Res.*, 2012, **19**, 3676-3687.

28. M. Šimšíková, M. Bartoš, P. Keša and T. Šikola, *Res. Bull.* submitted.

29. S. Liu, J. Tian, L. Wang, Y. Luo and X. Sun, *Catal. Sci. Technol.*, 2012, **2**, 339-344.

30. Y. Jiang, X.J. Wu, Q. Li, J. Li and D. Xu, *Nanotechnology*, 2011, **22**, 385601.

31. F. Tuinstra and J.L. Koenig, *J. Chem. Phys.*, 1970, **53**, 1126-1130.

32. Y. Guo, S. Guo, J. Ren, Y. Zhai, S. Dong and E. Wang, *ACS Nano*, 2010, **4**, 4001-4010.

33. S. Stankovich, D.A. Dikin, R.D. Piner, K.A. Kohlhaas, A. Kleinhammes, Y. Jia, Y. Wu, S.T. Nguyen and R.S. Ruoff, *Carbon*, 2007, **45**, 1558-1565.

34. J. Lee, S. Shim, B. Kim and H.S. Shin, *Chem. Eur. J.*, 2011, **17**, 2381-2387.

35. N.G. Sahoo, H. Bao, Y. Pan, M. Pal, M. Kakran, H. Kuo, F. Cheng, L. Li and L.P. Tan, *Chem. Commun.*, 2011, **47**, 5235-5237.

36. J. Shen, B. Yan, M. Shi, H. Ma, N. Li and M. Ye, *J. Mater. Chem.*, 2011, **21**, 3415-3421.

37. X. Huang, N. Hu, R. Gao, Y. Yu, Y. Wang, Z. Yang, E. S. W. Kong, H. Wei and Y. Zhang, *J. Mater. Chem.*, 2012, **22**, 22488-22495.

38. M. Baia, F. Toderas, L. Baia, D. Maniu and S. Astilean, *ChemPhysChem*, 2009, **10**, 1106-1111.

39. A. Komalam, L.G. Muraleegharan, S. Subburaj, S. Suseela, A. Babu and S. George, *Int. Nano Lett.,* 2012, **2**, 1-9.

40. Z.J. Jiang, C.Y. Liu and L.W. Sun, *J. Phys. Chem. B*, 2005, **109**, 1730-1735.

41. K.B. Narayanan and N. Sakthivel, N., *J. Hazard. Mater.*, 2011, **189***,* 519-525.

42. Y. He, L. Shaopu, L. Qin, L. Zhongfang and H. Xiaoli, *Sci. China Chem.*, 2005, **48**, 216-226.

43. M.M. Rhaman, F.R. Fronczek, D.R. Powell and M.A. Hossain, *Dalton Trans.*, 2014, **43**, 4618-4621.

44. P.V. Kamat, S. Barazzouk and S. Hotchandani, *Angew. Chem.*, 2002, **114**, 2888-2891.

45. Z. Zhu, R.H. Yang, M.X. You, X.L. Zhang, Y.R. Wu and W. Hong, *Anal. Bioanal. Chem.*, 2010, **396**, 73-83.

46. Y. Liu, C.Y. Liu and Y. Liu, *Appl. Surf. Sci.*, 2011, **257**, 5513-5518.

47. T. Huang and R.W. Murray, *Langmuir*, 2002, **18**, 7077-7081.

48. K. Bera, T. Ghosh and S. Basak, *J. Phys. Chem. C*, 2015, **119**, 1800-1808.

49. G. Raju, J. Capo, B.R. Lichtenstein, J.F. Cerda and R.L. Koder, *Tetrahedron Lett.*, 2012, **53**, 1201-1203.

50. F. Wang, M. Shao, L. Cheng, D. Chen, Y. Fu and D.D.D. Ma, *Mater. Res. Bull.*, 2009, **44**, 126-129.

51. V.K. Vidhu and D. Philip, *Micron*, 2014, **56**, 54-62.

52. R. Rajesh, S.S. Kumarb and R. Venkatesan, *New J. Chem.,* 2014, **38**, 1551-1558.

53. H. Lade, S. Govindwar and D. Paul, *Int. J. Environ. Res. Public Health*, 2015, **12**, 6894-6918.

54. H. Yan, X. Tao, Z. Yang, K. Li, H. Yang, A. Li and R. Cheng, *J. Hazard. Mater.*, 2014, **268**, 191-198.

55. S.T. Yang, S. Chen, Y. Chang, A. Cao, Y. Liu and H. Wang, *J. Colloid Interface Sci.* 2011, **359**, 24-29.

56. Z. Dong, D. Wang, X. Liu, X. Pei, Li. Chen and J. Jin, *J. Mater. Chem. A*, 2014, **2**, 5034

57. W. Zhang, C. Zhou, W. Zhou, A. Lei, Q. Zhang, Q. Wan, B. Zou, *Bull. Environ. Contam. Toxicol.*, 2011, **87**, 86-90.

58. D.C. Marcano, D.V. Kosynkin, J.M. Berlin, A. Sinitskii, Z. Sun, A. Slesarev, L.B. Aleman, W. Lu and J.M. Tour, *ACS Nano.*, 2010, **4**, 4806-4814.

HOOC

OH

OH

COOH

OH

GO

$+ HAuCl_4 . 3H_2O +$

green tea

rGO-AuNFs

$+ NaBH_4$

| 1 | 2 | 3 |

| 1 | 2 | 3 |

* 1 - safranin T, 2 - congo red, 3 - eosin Y

424x460mm (72 x 72 DPI)